

Cite this: *Chem. Commun.*, 2011, **47**, 4418–4420

www.rsc.org/chemcomm

## COMMUNICATION

## Amphiphilic porphyrin assembly as a highly selective chemosensor for organic mercury in water†

Bo-Wen Liu, Yong Chen, Bao-E Song and Yu Liu\*

Received 6th December 2010, Accepted 22nd February 2011

DOI: 10.1039/c0cc05413e

**Homogeneously sized nanoparticles were successfully constructed based on amphiphilic porphyrin-cholesterol arrays, showing unique spectral and colourimetric response to organic mercury in water, even in the presence of Hg<sup>2+</sup>.**

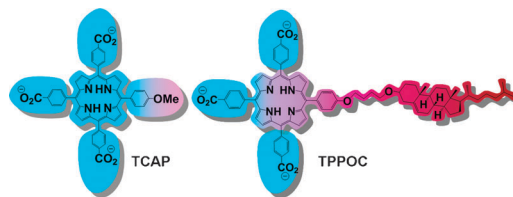
The high toxicity of mercury even at low concentrations, constitutes a significant detriment both to the environment and human health.<sup>1</sup> Typically, mercury exists in inorganic forms or as organic mercury compounds (RHg(II)<sup>+</sup>, R = Me, Et, Ph). As the most prevalent inorganic form, once entering the aquatic ecosystem, Hg<sup>2+</sup> is *in situ* biomethylated by microorganisms and converted into its organic form, which is then readily absorbed by fish and eventually accumulated through the trophic chain.<sup>2</sup> Compared with inorganic analogues, organic mercury species are much more neurotoxic and can easily penetrate the blood–brain barrier.<sup>3</sup> Thereby, the sensitive detection of organic mercury in aqueous systems has considerable diagnostic value. Generally, the detection of organic mercury is mainly achieved by chromatography techniques hyphenated with different element specific detectors; however, this method suffers from several inevitable limitations: high cost, complicated instrumentation and time-consuming sample pretreatment, that might cause sample contamination. Therefore, optical sensors have been regarded as one of the best options for the on-line and on-site detection of toxins in environmental and biological systems.<sup>4</sup> Recently, several chemosensors for organic mercury based on the mercury-induced desulfurization or ether cleavage were reported.<sup>5</sup> Since RHg(II)<sup>+</sup> is less thiophilic than Hg<sup>2+</sup>, especially in water, the development of an optical sensor capable of selective detection of organic mercury in the aquatic environment is still an unachievable goal by this route.

Herein, we successfully constructed a nanometre-scaled supra-molecular architecture through the self-assembly of a new tri-(*p*-carboxyphenyl)porphyrin-cholesterol dyad (TPPOC, Scheme 1) and comprehensively characterized its structure. Significantly, this supramolecular self-assembly with good water solubility,

exhibited a unique spectral response towards organic mercury, which could be readily observed visually or UV-vis spectroscopy, even in the presence of various competitive ions and aromatic compounds. This finding would enable our sensor as a convenient and highly efficient chemosensor for the detection of organic mercury in water.

TPPOC was synthesized in two steps with a total yield of 80% and fully characterized (Fig. S1–S4, ESI†), showing good solubility in aqueous solution. Both the concentration-dependent absorption and fluorescence behaviours (Fig. S7, S8†) by varying the concentration of TPPOC within the range from nM to μM revealed that it formed aggregates at quite a low concentration. Moreover, in the presence of 80% methanol, the Soret band of TPPOC appeared at 417 nm with intense absorption intensity<sup>6</sup> (Fig. S9a†); while in the absence of methanol, the Soret band hypochromatically shifted to 404 nm, together with the absorption intensity attenuating dramatically. Besides, the addition of methanol also led to a sharp fluorescence increase (Fig. S9b†). These phenomena jointly indicated a possible face-to-face aggregation of the anionic porphyrin heads *via* hydrophobic interactions and π–π stackings.<sup>7</sup> The critical assembly concentration (CAC) of TPPOC was determined to be 33.5 ± 7 nM by a reported method (Fig. S10†).<sup>8</sup> The absorption spectrum of tri(*p*-carboxyphenyl)-*p*-anisoleporphyrin (TCAP) synthesized as a reference compound, under comparable condition displayed an intense and sharp Soret band at 414 nm, and the addition of methanol caused no apparent changes (Fig. S11†), indicating that TCAP was molecularly dissolved.

A combined study by transmission electron microscopy (cryo-TEM), atomic force microscope (AFM) and dynamic light scattering (DLS) measurements was conducted to assess the morphology and size of the TPPOC aggregates. The cryo-TEM



**Scheme 1** Molecular structures of TCAP and TPPOC. Azure and ruby-red colours outline the most hydrophilic and hydrophobic part of this compound respectively.

Department of Chemistry, State Key Laboratory of Element-Organic Chemistry, Nankai University, Tianjin 300071, P. R. China.

E-mail: yuliu@nankai.edu.cn; Fax: (+86)22-2350-3625;

Tel: (+86)22-2350-3625

† Electronic supplementary information (ESI) available: Synthesis of TPPOC and TCAP, NMR, DLS, UV-vis and CAC measurements. See DOI: 10.1039/c0cc05413e

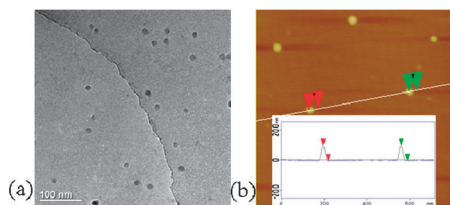


**Fig. 1** (a) Cryo-TEM and (b) AFM images of **TPPOC** aggregates.

images of **TPPOC** aggregates (Fig. 1a and Fig. S12†) displayed separated nanoparticles with a homogenous diameter of *ca.* 10 nm. In addition, the DLS experiment gave an average hydrodynamic radius as 10.6 nm with quite a narrow size distribution (Fig. S13†), also indicative of the formation of particles at nanoscale. The AFM image (Fig. 1b) at a relatively low concentration revealed that the average height of the particles was *ca.* 10 nm, which was consistent with the value of particle diameter obtained from TEM images.

After verifying the topology of **TPPOC** aggregates, we investigated their sensing abilities towards organic mercury.<sup>9</sup> Quantitative titration curves of **TPPOC** aggregates upon addition of phenylmercury,  $\text{PhHg(II)}^+$ , are shown in Fig. 2a. Upon the stepwise addition of  $\text{PhHg(II)}^+$ , the absorption maximum of **TPPOC** aggregates at 404 nm gradually decreased, accompanied by a slight red-shift of the absorption peaks, whilst a new absorption maximum appeared at 465 nm, and its intensity gradually increased with increasing the concentration of  $\text{PhHg(II)}^+$ . The absorption intensity values of **TPPOC** aggregates at 465 nm were plotted against the concentration of  $\text{PhHg(II)}^+$  (Fig. 2a, inset), showing a nearly linear variation within the concentration range from 500 nM to 18  $\mu\text{M}$  and an inflexion point at about 50  $\mu\text{M}$ , while the absorption of  $\text{PhHg(II)}^+$  was negligible within the concentration range of measurements (Fig. S14†). This phenomenon might refer to a complicated association of **TPPOC** aggregates with  $\text{PhHg(II)}^+$ . Additionally, the limit of detection (LOD value) of **TPPOC** aggregates towards  $\text{PhHg(II)}^+$  was calculated to be  $6.7 \times 10^{-7}$  M, (134 ppb Hg), which was close to or somewhat higher than those of colourimetric sensors for  $\text{Hg}^{2+}$  reported by the groups of Mirkin,<sup>10</sup> Yang<sup>11</sup> and Liu.<sup>12</sup> The absorption of **TPPOC** aggregates at 465 nm reached a maximum at 400 s after the addition of  $\text{PhHg(II)}^+$  (Fig. S15†). For comparison, we also conducted the UV-vis titrations of **TPPOC** in 80% MeOH–3% DMSO–CHES (Fig. S16†) and **TCAP** in 3%

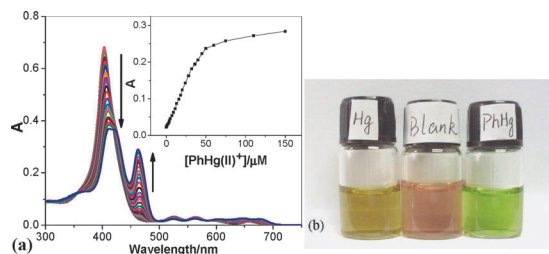


**Fig. 2** (a) UV-vis titration spectra of **TPPOC** (5  $\mu\text{M}$ ) upon addition of  $\text{PhHg(II)}^+$  (0–150  $\mu\text{M}$ ) in 3% DMSO–CHES (pH = 9.8, 10 mM). A tiny amount of DMSO was added to guarantee  $\text{PhHg(II)}^+$  completely dissolved in solution. The inset shows the absorbance intensity at 465 nm vs.  $[\text{PhHg(II)}^+]$ . (b) Colour changes of **TPPOC** (10  $\mu\text{M}$ ) upon addition of 5 equiv.  $\text{Hg}^{2+}$  or  $\text{PhHg(II)}^+$ .

DMSO–CHES (Fig. S17†) with  $\text{PhHg(II)}^+$ , respectively. It should be noted that both of the molecules remain in monomeric form under these conditions. The LOD values were determined to be more than 11 times and 46 times higher than that of the aggregates (Table 1), respectively.

Additionally, **TPPOC** aggregates also exhibited some spectral response to  $\text{Hg}^{2+}$ , but only as a shoulder appearing at 430 nm (Fig. S18†). Significantly, the spectral changes in the presence of mercury, could be readily distinguished visually. As seen in Fig. 2b, the solution of **TPPOC** aggregates was observed to be light pink, but changed to bright green or olive yellow in the presence of  $\text{PhHg(II)}^+$  or  $\text{Hg}^{2+}$ , respectively. These phenomena demonstrated not only the validity of **TPPOC** aggregates as an efficient chemosensor for organic mercury, but also the first probe reported, to the best of our knowledge, capable of discriminating organic and inorganic mercury species in water (Fig. S19†).

It is necessary to compare the sensing ability of **TPPOC** aggregates to other substances such as metal cations and aromatic compounds, since a very important characteristic feature of a sensor is its response to the species to be measured in the presence of other species. As seen in Fig. 3a, the absorption responses of **TPPOC** aggregates to various common monoaromatic pollutants, including benzene, toluene, nitrobenzene, chlorobenzene, fluorobenzene, phenol, aniline, benzoic acid, and benzyltrimethylammonium bromide (BAB), were investigated, but no appreciable spectral changes of **TPPOC** aggregates could be observed upon adding any of these compounds (Fig. S20†), regardless of latent  $\pi$ – $\pi$  and electrostatic interactions. The addition of another organic metal compound,  $\text{Ph}_2\text{Zn}$  did not have much influence on the absorption of the aggregates, either (Fig. S21†). Meanwhile, the **TPPOC** aggregates also showed substantial absorption changes, most of which were similar to that for  $\text{PhHg(II)}^+$  (Fig. S22†), for solutions containing  $\text{PhHg(II)}^+$  and various alkali earth metal ions ( $\text{Ba}^{2+}$ ,  $\text{Ca}^{2+}$  and  $\text{Mg}^{2+}$ ) or transition metal ions ( $\text{Pb}^{2+}$ ,  $\text{Cd}^{2+}$ ,  $\text{Co}^{2+}$ ,  $\text{Cu}^{2+}$ ,  $\text{Zn}^{2+}$ ,  $\text{Ni}^{2+}$ ,  $\text{Fe}^{2+}$ ,  $\text{Ag}^+$ ). Although the presence of excess  $\text{Mn}^{2+}$  or  $\text{Hg}^{2+}$  still gave rise to some absorption at 465 nm, it did not hamper the determination of  $\text{PhHg(II)}^+$  from the profile of the UV curve (Fig. S23†). The colourimetric experiments also gave similar results (Fig. 3b). In control experiments, the absorption of **TPPOC** monomers in 80% MeOH–3% DMSO–CHES was heavily affected by  $\text{Pb}^{2+}$  (Fig. S24†).<sup>13</sup> The absorption spectra of **TPPOC** at concentrations below the CAC value and upon addition of 100 equiv.  $\text{PhHg(II)}^+$  were recorded, but no apparent change could be observed (Fig. S25†). Moreover, the average hydrodynamic radius of **TPPOC** aggregates, measured by the DLS experiments, were nearly unchanged with the addition of  $\text{Hg}^{2+}$ , but increased to 17.1 nm in the presence of  $\text{PhHg(II)}^+$ . The ESI-MS experiments showed that in a dilute solution,

**Table 1** LOD values of **TCAP** and **TPPOC** under different conditions

|                                      | LOD/M (ppb Hg)              |
|--------------------------------------|-----------------------------|
| <b>TCAP</b> (3% DMSO–CHES)           | $3.1 \times 10^{-5}$ (6200) |
| <b>TPPOC</b> (80% MeOH–3% DMSO–CHES) | $7.7 \times 10^{-6}$ (1540) |
| <b>TPPOC</b> (3% DMSO–CHES)          | $6.7 \times 10^{-7}$ (134)  |

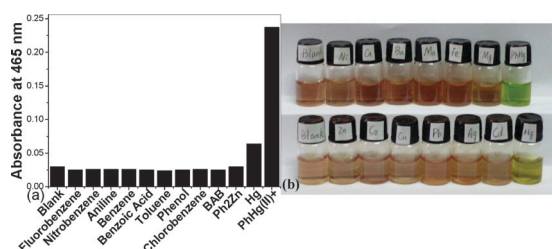


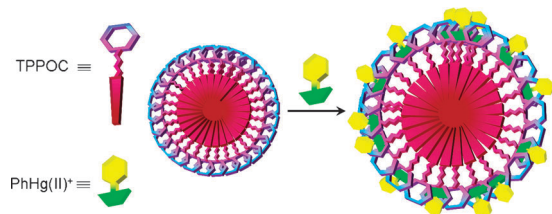
**Fig. 3** (a) Absorbance intensity of **TPPOC** (5  $\mu\text{M}$ ) at 465 nm, upon addition of 50  $\mu\text{M}$  monoaromatic pollutants,  $\text{Ph}_2\text{Zn}$ ,  $\text{Hg}^{2+}$  and  $\text{PhHg}(\text{II})^+$ , respectively. (b) Colourimetric images of **TPPOC** aggregates in the presence of  $\text{PhHg}(\text{II})^+$  or various metal ions.

only the  $m/z$  peak at 1479 assigned to the stoichiometric 1 : 1 complex could be observed (Fig. S26<sup>†</sup>), while at high concentration a  $m/z$  peak at 1340 assigned to the stoichiometric 2 : 1 complex, i.e.  $[\text{2TPPOC} + \text{PhHg}(\text{II})^+ - \text{2H}]^{2-}/2$ , also appeared (Fig. S27<sup>†</sup>).

For further elucidation of the possible sensing mechanism of **TPPOC** aggregates, we performed ROESY experiments to obtain more information about the interaction between the aggregates and  $\text{PhHg}(\text{II})^+$ . In the presence of  $\text{PhHg}(\text{II})^+$ , the cross-peaks (Fig. S28<sup>†</sup>, marked by circles) assigned to the NOE correlations of the phenyl group of  $\text{PhHg}(\text{II})^+$  with the cholesterol moiety of **TPPOC** clearly demonstrated that the lipophilic  $\text{PhHg}(\text{II})^+$  molecules were included in the hydrophobic interior of the **TPPOC** assembly, which also provided a better environment for the effective complexation between  $\text{PhHg}(\text{II})^+$  and the porphyrin moiety of **TPPOC** (Scheme 2).<sup>14,15</sup> This result was basically consistent with that of binding constants (Fig. S29, S30<sup>†</sup>), showing that **TPPOC** aggregates gave stronger binding ( $3.0 \times 10^4 \text{ M}^{-1}$ ) towards  $\text{PhHg}(\text{II})^+$  than the free **TPPOC** ( $4.4 \times 10^3 \text{ M}^{-1}$ ). Therefore, the sensing ability of **TPPOC** towards organic mercury was improved to the ppb level upon the formation of aggregates in the aqueous environment.

An important advantage of the detection method is the low-carbon recycling yield and facile regeneration of these self-assembled particles (Scheme S1<sup>†</sup>). The recycling rate is >90% (Fig. S31<sup>†</sup>).

In conclusion, the spontaneously assembled nanoparticles in water, comprised of porphyrin–cholesterol dyads, could selectively sense organic mercury with a good detection limit at ppb level, giving both the obvious spectral and colour changes. In addition, this chemosensor could be readily recycled under appropriate



**Scheme 2** The possible structure of nanoparticles based on **TPPOC** aggregates and its binding mode with organic mercury (yellow and green colors represent the phenyl and mercurial moieties, respectively). The organic mercury molecules concentrated inside were omitted for a clear view.

conditions. A preliminary study confirmed that this chemosensor presented the sensing ability to another important organic mercury species, methylmercury,  $\text{MeHg}(\text{II})^+$  (Fig. S32<sup>†</sup>). These results may not only have important applications in the current detection techniques for organic mercury species, whereas may also open the door for the design of functional nano-scaled materials based on self-assembled supramolecular systems. Studies on the selective sensing of **TPPOC** and improved homologues to methylmercury are still in progress.

This work was financially supported by 973 Program (2011CB932500) and NNSFC (No. 20932004 and 91027007). We are also grateful to Prof. X.-P. Yan of Nankai University for his kind help.

## Notes and references

- (a) W. Sekowski, L. H. Malkas, Y. Wei and R. J. Hickey, *Toxicol. Appl. Pharmacol.*, 1997, **145**, 268–276; (b) W. H. Organization, *Environmental Health Criteria 118: Inorganic Mercury*, World Health Organization, Geneva, 1991.
- (a) T. W. Clarkson, L. Magos and G. J. Myers, *N. Engl. J. Med.*, 2003, **349**, 1731–1737; (b) F. M. M. Morel, A. M. L. Kraepiel and M. Amyot, *Annu. Rev. Ecol. Syst.*, 1998, **29**, 543–566.
- M. Aschner and J. L. Aschner, *Neurosci. Biobehav. Rev.*, 1990, **14**, 169–176.
- (a) M. I. J. Stich, L. H. Fischer and O. S. Wolfbeis, *Chem. Soc. Rev.*, 2010, **39**, 3102–3114; (b) E. M. Nolan and S. J. Lippard, *Chem. Rev.*, 2008, **108**, 3443–3480.
- (a) O. del Campo, A. Carbayo, J. V. Cuevas, A. Muñoz, G. García-Herbosa, D. Moreno, E. Ballesteros, S. Basurto, T. Gómez and T. Torroba, *Chem. Commun.*, 2008, 4576–4578; (b) M. Santra, D. Ryu, A. Chatterjee, S.-K. Ko, I. Shin and K. H. Ahn, *Chem. Commun.*, 2009, 2115–2117; (c) Y.-K. Yang, S.-K. Ko, I. Shin and J. Tae, *Org. Biomol. Chem.*, 2009, **7**, 4590–4593; (d) H. Wang and W.-H. Chan, *Tetrahedron*, 2007, **63**, 8825–8830; (e) E. Climent, M. D. Marcos, R. Martínez-Mañez, F. Sancenón, J. Soto, K. Rurack and P. Amorós, *Angew. Chem., Int. Ed.*, 2009, **48**, 8519–8522; (f) X.-Q. Chen, K.-H. Baek, Y. Kim, S.-J. Kim, I. Shin and J. Yoon, *Tetrahedron*, 2010, **66**, 4016–4021; (g) M. Park, S. Seo, I. S. Lee and J. H. Jung, *Chem. Commun.*, 2010, **46**, 4478–4480.
- M. Y. Choi, J. A. Pollard, M. A. Webb and J. L. McHale, *J. Am. Chem. Soc.*, 2003, **125**, 810–820.
- F. Helmich, C. C. Lee, M. M. L. Nieuwenhuizen, J. C. Gielen, P. C. M. Christianen, A. Larsen, G. Fytas, P. E. L. G. Leclère, A. P. H. J. Schenning and E. W. Meijer, *Angew. Chem., Int. Ed.*, 2010, **49**, 3939–3942.
- S. Tomas and L. Milanese, *J. Am. Chem. Soc.*, 2009, **131**, 6618–6623.
- While organic mercury species are highly toxic,  $\text{PhHg}(\text{II})^+$  may be used relatively safely, owing to its low volatility. A water-soluble phenylmercury derivative, *p*-hydroxymercuribenzoate, has served as a model for mechanistic investigation of organic mercury protonolysis by organo-mercurial lyase. See: K. E. Pitts and A. O. Summers, *Biochemistry*, 2002, **41**, 10287–10296.
- J.-S. Lee, M. S. Han and C. A. Mirkin, *Angew. Chem., Int. Ed.*, 2007, **46**, 4093–4096.
- Y. Wang, F. Yang and X. R. Yang, *ACS Appl. Mater. Interfaces*, 2010, **2**, 339–342.
- X. Xue, F. Wang and X. Liu, *J. Am. Chem. Soc.*, 2008, **130**, 3244–3245.
- K. Kilian and K. Pyrzyńska, *Talanta*, 2003, **60**, 669–678.
- K.-T. Chen, F.-A. Yang, J.-H. Chen, S.-S. Wang and J.-Y. Tung, *Polyhedron*, 2008, **27**, 2216–2220.
- (a) Y. Li, Y. Jiang and X.-P. Yan, *Anal. Chem.*, 2006, **78**, 6115–6120; (b) G. Chirico, M. Collini, L. D'Alfonso, F. Denat, Y. A. Diaz-Fernandez, L. Pasotti, Y. Roussel, N. Sok and P. Pallavicini, *ChemPhysChem*, 2008, **9**, 1729–1737.